Mathematical model for dynamic force analysis of printed circuit boards

Mathematical model for dynamic force analysis of printed circuit boards

I.I. Kovtun, J.M. Boiko, S.A. Petrashchuk

Khmelnytsky National University, Khmelnitsky, 29016, Ukraine

E-Mail: dr.igorkovtun@gmail.com

Abstract. Mathematical model for dynamic force analysis of printed circuit boards has been designed to calculate dynamic deformations and stresses in printed circuit boards and assess their dynamic strength and rigidity. The represented model describes a printed circuit board as a separate oscillatory system, which is simulated as prismatic beam set on two oscillating supports. Simulation and assessment of stress and deflection in printed circuit boards and obtaining their amplitude frequency responses provided recommendations, which ensure strength and stiffness of printed circuit boards subjected to dynamic loads.

1. Introduction

Mathematical model for dynamic force analysis of printed circuit boards (PCB) has been designed to calculate dynamic deformations and stresses in printed circuit boards and assess their dynamic strength and stiffness. The represented model describes printed circuit board as the separate oscillatory system. Unlike the previous model published in [1,2], the printed circuit board is no longer represented by a point particle (mass). In this case it is represented by prismatic beam or a plate.

The initial choice of the beam for printed circuit board simulation is explained by the fact that cylindrical bending of a board can be considered as bending of the set of beam-strips, having rectangular cross-section imaginary cut out of this board in transverse direction, thus the stress and strain calculation of such beam-strips can be performed by using conventional methods applied in strength of materials [3] (internal forces and moments diagrams, stress and strain calculation, etc.).

Numerous publications devoted to stresses assessment [4] and mechanical strength control [5] for electronic packages, and in particular to printed circuit boards [6], subjected to bending and shear forces [7] and undergoing dynamic deformations [8], performance of dynamic analysis [9] and reliability [10] using vibration reduction design [11] and vibration suppression methods [12] indicate of insufficient strength and reliability of modern electronic packages explored in harsh conditions of variety of impacts including mechanical shocks and vibration. Mathematical modeling represented in this paper is aimed at dynamic force analysis of printed circuit boards in order to eliminate or reduce dynamic stress to an acceptable level and to provide strength and reliability in design of printed circuit boards subjected to vibration.

2. Dynamic loads on the beam

Figure 1 represents the dynamic load on the beam with concentrated mass *m*. Such representation assumes the beam mass negligibly small in comparison with concentrated mass. Electronic components, or a group of components, whose mass exceeds mass of the board, and in this way creates an uneven load distribution of oscillatory system, are considered to be the concentrated mass.

The beam rests on two points O and O' representing pinned support (with one degree of freedom) and roller (with two degrees of freedom) correspondently (to simplify the scheme types of supports are not shown in figure 1), through which the beam is exposed to external force.

With respect to inertial frame of reference, which can be represented by supports of the shaker, oscillation of mass m proceeds with acceleration a_1, due to kinematic excitation generated by oscillations of the beam ends, to which dynamic force is applied and which move with given acceleration a_0. The difference in these accelerations, taking into account their directions, is $\Delta a = a_1 - a_0$ and represents acceleration of the mass m with respect to supports O and O', which introduce non-inertial frame of reference. Taking into account the non-inertial frame of reference and all forces acting on the mass m: force of inertia; fictitious force of inertia; elastic force F_k and damping force F_c, the equation of motion for mass m is expressed as:

$$\ddot{f} + \omega_0^2 f + 2l\dot{f} = -a_0, \tag{1}$$

where $f = f(t)$ – required function of mass m displacement.

The oscillation is generated by the shaker, whose table performs the vertical movement (parallel to Z axis) described by harmonic oscillations:

$$z_0(t) = Z_0 \sin(\omega t), \tag{2}$$

where Z_0 – amplitude; $\omega = 2\pi f$ – angular frequency, f – frequency; t – time; φ – phase of oscillations.

Then $a_0 = -Z_0\omega^2 \sin(\omega t)$ and differential equation (1) is obtained identically to equation represented in [1,2] so its solution has expression identical to [1,2]:

$$f(t) = Z_0\omega^2((\omega_0{}^2 - \omega^2)^2 + (2l\omega)^2)^{-1/2} \cdot \sin\left(\omega t - \operatorname{arcctg}\left(\frac{\omega_0{}^2 - \omega^2}{2l\omega}\right)\right), \tag{3}$$

or in brief notation:

$$f(t) = A \sin(\omega t - \varphi). \tag{4}$$

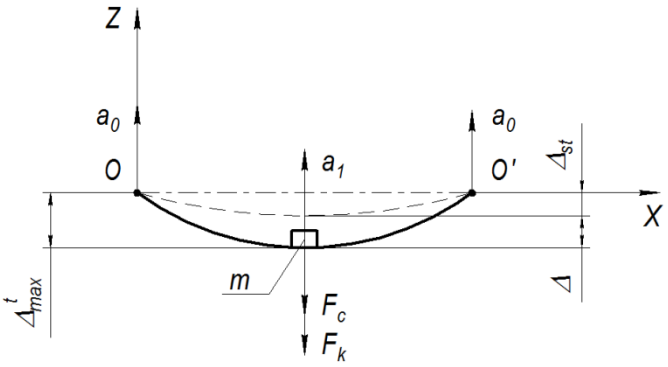

Figure 1. Dynamic loads on the beam with concentrated mass

3. Dynamic net force acting on the board

As shown in (figure 1), function (4) describes deflection Δ of the beam, which occurs with respect to static equilibrium position of the oscillation system Δ_{st} :

$$\Delta_{st} = \frac{mg}{k} = \frac{g}{\omega_0^2}, \tag{5}$$

where k – stiffness; ω_0 – natural frequency; g – gravity.

Taking into account static equilibrium position the total deflection is Δ^t_{max}:

$$\Delta^t_{max} = A + \Delta_{st}. \tag{6}$$

where A – amplitude of oscillations that can always be expressed by static deflection A_{st} and dynamic coefficient k_{dyn}:

$$A = A_{st} \cdot k_{dyn}. \tag{7}$$

Static deflection (displacement) of the system produced by maximal value of dynamic force in its direction is determined from equation (1) for $f''(t) = 0$ and $f'(t) = 0$:

$$A_{st} = \frac{Z_0\omega^2}{{\omega_0}^2}. \tag{8}$$

Dynamic coefficient:

$$k_{dyn} = \left(\left(1 - \frac{\omega^2}{{\omega_0}^2}\right)^2 + \frac{(2l\omega)^2}{{\omega_0}^4}\right)^{-1/2}. \tag{9}$$

Total deflection is produced by the net force P representing force of inertia P_i and gravity P_{st} (weight) of the mass m, thus:

$$P = P_i + P_{st} = \frac{\Delta^{\Pi}_{max}}{\delta}, \tag{10}$$

where δ – flexibility of the beam in direction of force P.

The flexibility of the beam in direction of actual force P (figure 2) is convenient to find by its substitution with a single force $P_1 = 1$ and defined by Mohr's integral:

$$\delta = \sum_k \int_{x_k} \frac{\left(M_k^1\right)^2}{EJ} dx, \tag{11}$$

where k – number of the load section; x_k – length; M_k^1 – internal bending moment (table 1) in the direction and from the action of single force P_1; E and J – Young's modulus and moment of inertia of cross-sectional area of the beam respectively.

The flexibility formula (11) has been obtained according to hypothesis that fibers in the beam do not produce pressure on each other, what means that stress in direction perpendicular to the axis of the beam equals zero. Therefore, consideration of only internal bending moments is sufficient, while the action of internal transverse forces can be neglected.

Using the load application scheme given in figure 2 and formula (11) provides formula for flexibility of the beam at the point of single force application:

$$\delta = \frac{x^2(x-l)^2}{3Ejl}. \tag{12}$$

Determining flexibility (12) also allows calculating natural (resonant) frequency ω_0 of the printed circuit boards (beam) according to the formula:

$$\omega_0 = (\delta m)^{-1/2}. \tag{13}$$

According to formulas (10) and (5 - 9) the expression for the equivalent force P is:

$$P = Z_0\omega^2 m \cdot \left(\left(1 - \frac{\omega^2}{{\omega_0}^2}\right)^2 + \frac{c^2\omega^2}{m^2{\omega_0}^4}\right)^{-1/2} + mg. \tag{14}$$

4. Strength assessment

Strength assessment is performed by using the maximal total normal stress defined by bending formula of the beam:

$$\sigma^{\Pi}_{max} = \frac{M_{max}}{W}, \tag{15}$$

where M_{max} – maximal internal bending moment; W – axial moment of resistance, which for a rectangular cross section is determined by the formula:

$$W = \frac{bh^2}{6}, \tag{16}$$

where b – width; h – thickness of the beam.

Maximal internal bending moment corresponds to bending moment produced by the equivalent force P in the cross section of the beam with coordinate x, as shown in the diagram of moments (figure 2), and is defined as:

$$M_{max} = P \cdot x\left(1 - \frac{x}{l}\right). \tag{17}$$

The use of formulas (14 - 17) provides stress estimation and strength assessment of printed circuit boards represented by a beam with concentrated mass in specified range of oscillation frequencies.

5. Stiffness assessment

Stiffness assessment of printed circuit boards is proposed to perform by the value of maximal displacements (deflections) of the board. Noteworthy is that largest deflection of a beam coincides with spot of application of acting force only when the force is applied in the middle point of the beam. In the case when the concentrated mass, as well as correspondent force of inertia, are not in the middle, the largest deflection of a beam will not coincide with the place of force application. In any case finding maximal deflection is critical to assess the stiffness, the vibration characteristics of a structure and the risk of collisions and impacts with other (adjacent) structural elements of the housing or printed circuit boards.

To determine maximal deflection, in accordance to Mohr's method [3], the load application scheme (figure 3) and bending moments diagrams produced by the actual force *P* acting on the body and single force $X_1 = 1$ have been introduced. Among deflections Δ_{ij} shown in (figure 3) produced in direction of force "i" and by the action of force "j", the deflection Δ_{1P} is required, which is deflection in direction of force X_1 from the action of force *P*. This deflection can be found from equality of external and internal virtual work:

$$W_{1P} = W_{1P}^{B},$$

produced by the force X_1 in direction on displacement Δ_{1P}:

$$\Delta_{1P} = \sum_k \int_x \frac{M_k^1 \cdot M_k^P}{EJ} dx, \tag{18}$$

where M_k^1 – internal bending moment in direction and from the action of the single force X_1; M_k^P – internal bending moment from the action of external load *P* in direction of the single force X_1.

Expressions of functions for internal bending moments obtained using the method of cross sections are represented in table 1.

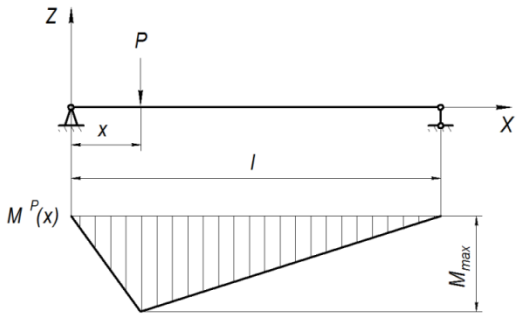

Figure 2. Net force application and bending moment diagram on the beam

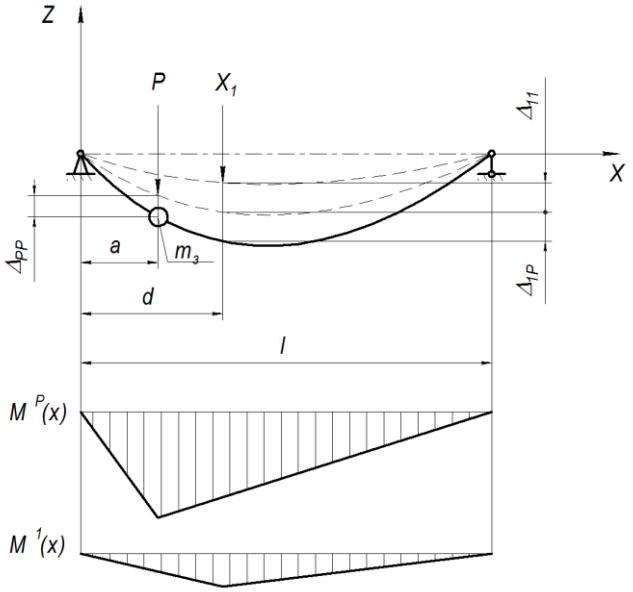

Figure 3. Loads and diagrams of bending moments produced by the actual and single forces

Table 1. Internal moments in the load sections on the beam

Load sections	$0 \le x \le a$	$a \le x \le d$	$d \le x \le l$
$M_1^1(x)$	$x\left(1-\frac{d}{l}\right)$	$x\left(1-\frac{d}{l}\right)$	$d\left(1-\frac{x}{l}\right)$
$M_P^1(x)$	$Px\left(1-\frac{a}{l}\right)$	$Pa\left(1-\frac{x}{l}\right)$	$Pa\left(1-\frac{x}{l}\right)$

Deflection of the beam (18) produced by force P in direction of force X_1 was expressed as function of linear coordinate d along the axis X of the beam. To make the record more convenient variable d was substituted with x, hereby the function of argument x is expressed as:

$$\Delta_{1P}(x) = \frac{Pa(x-l)(x^2-2lx+a^2)}{6EJl}. \quad (19)$$

The function (19) domain when $a \leq l/2$ represents the interval $a \leq x \leq l$, which provides the section with maximal deflection (figure 3).

The function (19) extremum corresponds to maximal deflection of the beam by the argument $x_0 = l - \frac{\sqrt{3}}{3}\sqrt{l^2 - a^2}$:

$$\Delta_{1P}^{max}(x_0) = \frac{\sqrt{3}Pa(l^2-a^2)^{\frac{3}{2}}}{27EJl}, \quad (20)$$

which is also evident from the graph representing $\Delta_{1P}(x)$ (figure 4, a). Deflection in this coordinate is used for beam stiffness assessment against its threshold limit value that is determined experimentally.

Another method to determine deflection of the beam is by using the approximate differential equation of curved axis of the beam [3]:

$$EJ\Delta''(x) = M(x). \quad (21)$$

Finding deflection considers the same load application scheme (figure 3) but with an exclusion for the use of the single force X_1. The maximal deflection obviously lays within the load section $a \leq x \leq l$. Double integration of differential equation (21) with substituting functions of internal moments obtained in table 1 results in deflection equation:

$$EJ\Delta_1(x) = \frac{Pax^2}{2} - \frac{Pax^3}{6l} + C_1x + D_1. \quad (22)$$

Double integration of equation (21) in the section $0 \leq x \leq a$ gives:

$$EJ\Delta_2(x) = \frac{Px^3}{6}(1 - \frac{a}{l}) + C_2x + D_2. \quad (23)$$

Integration constants C_1, D_1 and C_2, D_2 are found by consideration of displacements in characteristic points of the beam in both sections: $\Delta_2(0) = 0$; 2) $\Delta_1(l) = 0$; 3) $\Delta_1(a) = \Delta_2(a)$.

Then $D_1 = 0$ and $C_1 = -\frac{P \cdot a \cdot l}{3}$.

The equation of deflection of the beam in the section $a \leq x \leq l$ is expressed as:

$$\Delta(x) = \frac{Pa(x-l)(x^2-2lx)}{6lEJ}. \quad (24)$$

The extremum of function (24) corresponds to maximal deflection of the beam by the argument $x_0 = l - \frac{\sqrt{3}}{3}l$:

$$\Delta_{max}(x_0) = \frac{\sqrt{3}Pal^2}{27EJ}, \quad (25)$$

which is also evident from the graph of function $\Delta(x)$ represented in figure 4, a.

Comparative analysis of formulas (19) and (24) indicates insignificant difference in deflections, which reaches maximum when $a \to l/2$ (figure 4, b), although the first formula is characterized by higher accuracy of calculation. Analysis of formulas (20) and (25) to calculate maximal deflections shows that they are close to the deflection in the middle point on the beam and even in the most unfavorable case when $a \to 0$ the difference between them does not exceed 3%. Therefore the stiffness assessment, without significant loss of accuracy, may be performed by the value of deflection in the middle point on researched structure represented as a beam:

$$\Delta_{1P}^{max}(x_0) \approx \Delta_{max}(x_0) \approx \Delta_{mid}\left(\frac{l}{2}\right). \quad (26)$$

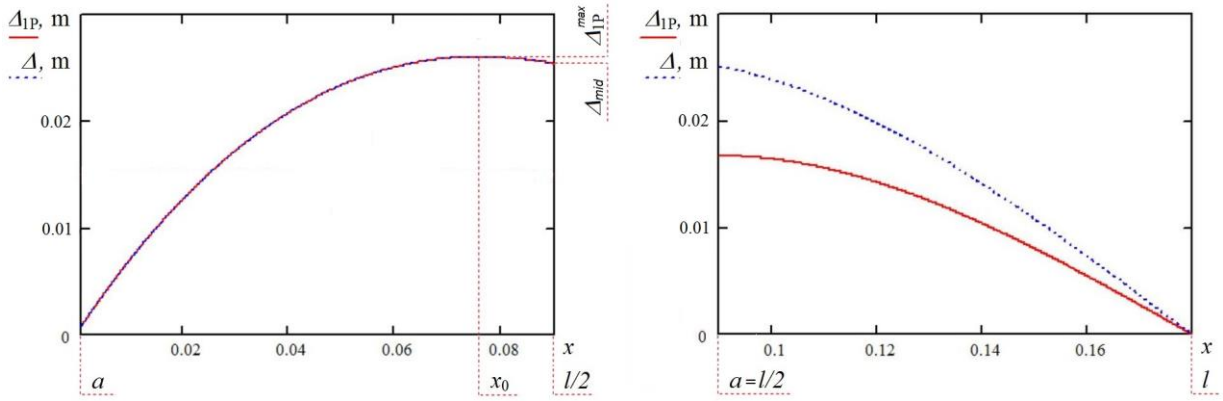

a) b)

Figure 4. The graph of deflection function on the beam

6. Simulation and strength and stiffness analysis of printed circuit boards

Simulation and analysis of maximal total normal stress and deflection was conducted for PCB samples with following characteristics: dimensions – 180×50×1.5 mm; the substrate material – fiberglass CAST-V, Young's modulus E = 14 GPa, density ρ = 1600 kg/m^3, ultimate strength σ_{fg} = 160-300 MPa; solder joints made by POS-40 solder with ultimate strength σ_{sld} = 40 MPa; damping found experimentally [2,13,14] ξ = 10.96 1/s; mass of electronic component (concentrated mass) m = 50 g; electronic component is mounted in the middle point of PCB.

Acceptable stress of the whole PCB structure is determined by ultimate strength of its structural element whose strength has lowest value. As shown in [15-18] soldered joints belong to such elements. Inaccuracy of ultimate strength for the solder, associated with design and technology of the joint, is taken into account by the safety factor n = 2.5, which limits ultimate stress within proportionality section on tensile diagram of the solder and does not reduce strength of the solder joint. Thus, the acceptable stress value of PCB is determined by formula [16-17,19]:

$$[\sigma] = \frac{\sigma_{sld}}{n} = 16 \text{ MPa}. \quad (27)$$

In the simulation PCB was subjected to dynamic load as shown in figure 1 with oscillation amplitude Z_0 = 1 mm. Figure 5 demonstrates amplitude frequency response of maximal total normal stress and deflection in PCB.

The amplitude frequency response of maximal total normal stress $\sigma(\omega)$ indicates the resonance at angular frequency ω_0 = 180.2 rad/s (28.67 Hz). Using graph (figure 5, a) allowed to reveal frequency ranges in which actual stress complies with ultimate strength limit: before resonance range: 0 - 160.8 rad/s and after resonance range: from 208.9 rad/s and higher. In frequency range near resonance actual stress is potentially destructive. Thus, recommendation was given for acceptable operating ranges of vibration frequencies, although their regulation is not always achievable in practice.

The amplitude frequency response of maximal deflections (figure 5, b) expressed as:

$$\Delta(\omega) = \frac{P(\omega)l^3}{48EI}, \quad (28)$$

demonstrates resonance at the same angular frequency ω_0 = 180.2 rad/s.

Acceptable deflection of PCB can be determined by using acceptable operating ranges of vibration frequencies found for maximal total normal stress (figure 5, b), then $\Delta \approx 4$ mm. Nevertheless acceptable deflection may be specified by experimental method for acceptable limit specification of PCB warpage introduced in [15], then $\Delta' = 5$ mm. As shown in figure 5, b this acceptable deflection allows even expanding the operating frequency range up to 0 - 164.2 rad/s and from 202.1 rad/s and higher without violating the stiffness condition and experimentally proven strength condition.

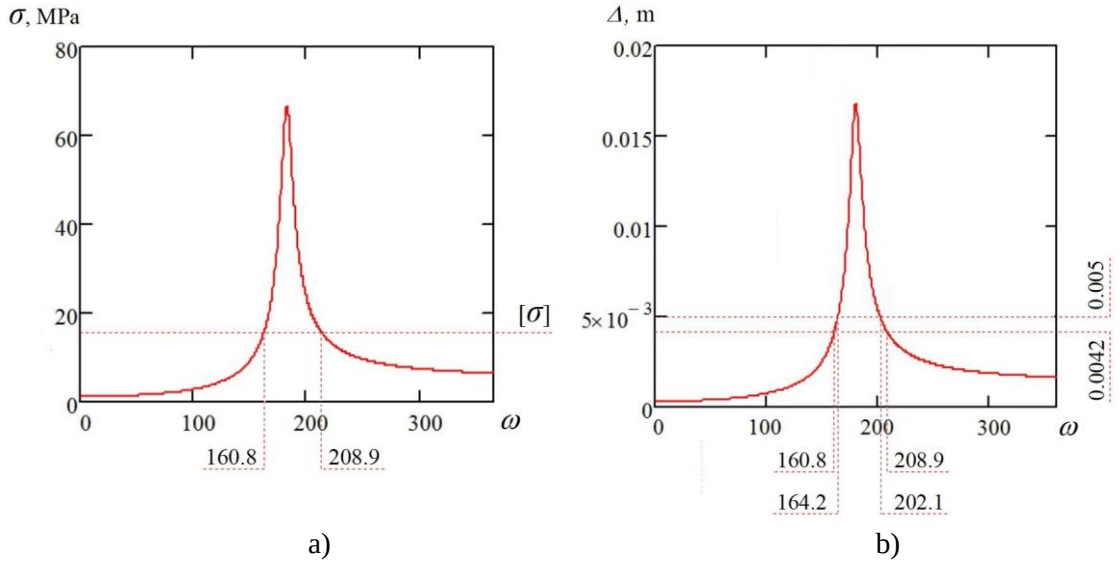

a) b)

Figure 5. Amplitude frequency response of maximal total normal stress and deflection in PCB

The undoubtedly desirable aim of the research would be to provide strength and stiffness of printed circuit boards even in conditions of resonant excitation without reference to a specific range of vibration frequencies. This research is to be in objective for the further publications.

7. Conclusions

Mathematical model for dynamic force analysis of printed circuit boards has been designed to calculate dynamic deformations and stresses in printed circuit boards and assess their dynamic strength and stiffness. The represented model describes a printed circuit board as a separate oscillatory system, which is, in this case, simulated as prismatic beam rested on two oscillating supports.

The simulation and analysis of maximal total normal stress and deflection of printed circuit boards and obtaining their amplitude frequency responses provided recommendations for acceptable operating ranges of vibration frequencies, which ensure strength and stiffness of printed circuit boards subjected to dynamic loads.

8. References

[1] Boiko J, Kovtun I and Petrashchuk S 2017 Vibration transmission in electronic packages having structurally complex design *Proc. IEEE First Ukraine Conf. on Electrical and Computer Engineering (UKRCON) (Kiev)* pp. 514-517, https://doi.org/10.1109/ukrcon.2017.8100294.

[2] Kovtun, I., Boiko, J., Petrashchuk, S., Kałaczyński, T. 2018 *Theory and practice of vibration analysis in electronic packages /17th International Conference Diagnostics of Machines and Vehicles. MATEC Web Conf.* (eISSN: 2261-236X), 182, 02015 (2018) – 10 p.

[3] G.S. Pisarenko, V.A. Agarev. Strength of materials. *Kiev: Technika*, 1967, 792 pp.

[4] Cevdet N I et al., 2016 *Stresses in Microelectronic Circuits in Reference Module in Materials Science and Materials Engineering* (Elsevier), doi.org/10.1016/B978-0-12-803581-8.01817-8.

[5] Kiilunen J and Frisk L 2017 The mechanical strength of microvias in reflow cycling and environmental aging *Proc. 21st European Microelectronics and Packaging Conference (EMPC) & Exhibition* (Warsaw) pp. 1-6, https://doi: 10.23919/EMPC.2017.8346871.

[6] Meng J and Dasgupta A 2017 Influence of Secondary Impact on Printed Wiring Assemblies—Part II: Competing Failure Modes in Surface Mount Components *J. Electron. Packag*. **139**(3): 031001, https://doi.org/10.1115/1.4036187.

[7] Loon K T et al., 2019 Modeling the Elastic Behavior of an Industrial Printed Circuit Board Under Bending and Shear *in IEEE Trans. on Components, Packag. and Manufac. Technology* **9**(4) pp. 669-676, https://doi: 10.1109/TCPMT.2018.2882575.
[8] Wong E-H and Mai Y-W 2015 *10 - Dynamic deformation of a printed circuit board in drop-shock in Robust Design of Microelectronics Assemblies Against Mechanical Shock, Temperature and Moisture* (Woodhead Publishing) pp. 327-378, doi.org/10.1016/B978-1-84569-528-6.00010-1.
[9] Allaparthi M et al., 2018 Three-dimensional finite element dynamic analysis for micro- drilling of multi-layered printed circuit board *Materials Today: Proc.* 5(2) pp. 7019-7028, doi.org/10.1016/j.matpr.2017.11.365.
[10] Kim Y K et al., 2020 Analyses on the large size PBGA packaging reliability under random vibrations for space applications *Microelectronics Reliability* **109** 113654, doi.org/10.1016/j.microrel.2020.113654.
[11] Xiao W et al., 2020 Vibration reduction design of extension housing for printed circuit board based on particle damping materials *Applied Acoustics* **168** 107434, doi.org/10.1016/j.apacoust.2020.107434.
[12] Veeramuthuvel P, Sairajan K K and Shankar K 2016 Vibration suppression of printed circuit boards using an external particle damper *J. of Sound and Vibration* **366** pp 98-116, doi.org/10.1016/j.jsv.2015.12.034.
[13] I. Kovtun, J. Boiko, S. Petrashchuk 2018 Identification of Natural Frequency and form of Oscillation for Electronic Packages Subjected to Vibration *Proceedings 2018 IEEE 38th International Conference on Electronics and Nanotechnology (ELNANO)*, 2018. – P. 621-626.
[14] I. Kovtun, J. Boiko, S. Petrashchuk 2019 Assessing Enclosure Case Design on Excitation and Transmission of Vibration in Electronic Packages *Proceedings Proc. IEEE 2nd Ukraine Conference on Electrical and Computer Engineering (UKRCON)*, Lviv, 2019. – P. 265-270.
[15] Kovtun I et al., 2016 Effects of the strain transmission from the main board to the installed electronic components *Mechanika*. – Kaunas : KTU, 2016. – Vol 22 № 6 (2016). – P: 494–489. ISSN 1392–1207, doi.org/10.5755/j01.mech.22.6.16891.
[16] Kovtun I, Boiko J and Petrashchuk S 2017 Nondestructive strength diagnostics of solder joints on printed circuit boards *Proc. IEEE Int. Conf. on Inform. and Telecom. Technolog. and Radio Electronics (UkrMiCo)* (*Odessa*) pp. 1-4, https://doi.org/10.1109/ukrmico.2017.8095401.
[17] I. Kovtun, V. Royzman, A. Voznyak 2018 Acoustic emission diagnostics of solder joints on printed circuit boards *Quality and Reliability of Technical Systems: Theory and Practice. JVE Book Series on Vibroengineering. Volume 2. JVE International Ltd*. – Vilnius, Lithuania. 2018. – P. 214-229. ISSN 2351-5260.
[18] Suhir E et al., 2019 Elevated Standoff Heights of Solder Joint Interconnections Can Result in Appreciable Stress and Warpage Relief *J. of Microelectronics and Electron. Packag.* **16**(1) pp. 13–20, doi.org/10.4071/imaps.735566.
[19] Kovtun I I, Boiko J M and Petrashchuk S A 2019 Reliability Improvement of Printed Circuit Boards by Designing Methods for Solder Joint Technical Diagnostics with Application of Acoustic Emission Method *Visnyk NTUU KPI Seriia-Radiotekhnika Radioaparatobuduvannia* **79** pp. 60-70, https://doi.org/10.20535/RADAP.2019.79.60-70.